EAI Endorsed Transactions
on Energy Web
Research Article EAI.EU

Switched capacitor voltage boost converter for BLDC motor speed control of electric vehicles

Srinivasan P[1,*], Murali Krishna K[1], Roshan M[1], Nissy Joseph[1]

[1]Department of Electrical and Electronics Engineering, SRM Institute of Science and Technology, Ramapuram, Chennai, India.
*Corresponding author: srinivasp808@gmail.com

Abstract

BLDC motors are extensively used in various industries, including CNC machine tools, industrial robots, and electric vehicles. Because of their compact size, high efficiency, high torque-to-power ratios, and low maintenance requirements due to their brushless operation, BLDC motors are the backbone of many industrial automation systems. However, they pose significant challenges when it comes to speed control. In this study, the speed of BLDC motors is controlled by PI-based speed controllers. In the described method, the BLDC motor is commutated using Hall Effect sensors. A proposed approach uses PI to regulate the speed of BLDC motors in an open-loop PWM method. The speed-controlled BLDC motor is analysed using MATLAB/simulink. The hardware of the proposed system is also implemented.

Keywords: Switched capacitor, DC-DC converters, BLDC motor, H6 VSI, BLDC Motor.

Received on 12 February 2024, accepted on 25 May 2024, published on 3 July 2024

doi: 10.4108/ew.6036

1. Introduction

The creation of efficient and reliable charging infrastructure is crucial, given the increasing adoption of electric cars (EVs) as a sustainable transportation mode. The motor is one of the many components that comprise an electric vehicle, and due to its superior torque characteristics and high efficiency, the BLDC has become the preferred motor for propulsion. According to a report, operating an electric car is less expensive than operating a conventional gasoline-powered car. Overall fuel costs are reduced because electricity is generally less expensive than gasoline or diesel. Since their components are less expensive than those of conventional cars, EVs also require less maintenance. It has been said that one of the main reasons electric cars are becoming increasingly popular is the expansion of the infrastructure for charging them. Fast-charging station expansion has further shortened car charging times, making EVs more suitable for long-distance driving. For electric vehicles (EVs), efficient battery charging is of utmost importance since it affects the vehicle's overall performance, driving range, and user experience. The battery's capacity and efficiency determine an electric car's driving range. The growing demand for electric vehicles (EVs) has led to significant advancements in motor technology, with BLDC emerging as a leading choice for EV propulsion systems. BLDC motors offer excellent torque characteristics, are compact and efficient, and are well-suited to electric vehicle applications. BLDC motors' high torque density and minimal controller requirements make them attractive for use in various electric vehicle applications. In the existing system, the DC link voltage needs to be greater than the input voltage, which is either DC or AC. Commercial traction electric propulsion typically uses one of these two layouts for applications. When the available DC voltage is limited, two batteries are used. One is used to power a two-level converter directly, while the other powers a DC-DC intermediate stage inverter [1]. A proportionally significant choke will arise from the DC-DC converter's power rating matching the battery's power. The drawback of this system is that the inductor is costly and bulky. We present a simulation of the proposed system that incorporates substantial hardware research and demonstrates how the speed management of the BLDC drive can be improved [2]. The proposed technique utilizes variable DC-link voltage regulation and pulse-width modulation technologies. The experimental validation of the BLDC drive has been reported.

2. Methodology

This research suggests a novel switched-capacitor power converter for DC-DC power conversion. Unlike the traditional boost converter, the SC converter is distinctive due to its use of a switched-capacitor circuit which is linked to the power source and increased with the main converter circuit [3]. The SC converter has the potential to reduce expenses, raise power density, reduce the number of components, and lift or cut down voltage. The output with an upgrade is transferred into a voltage source inverter (H6) for motor driving applications. The control mechanism, as seen, in figure 1a, ensures consistent performance in a variety of settings [4-6].

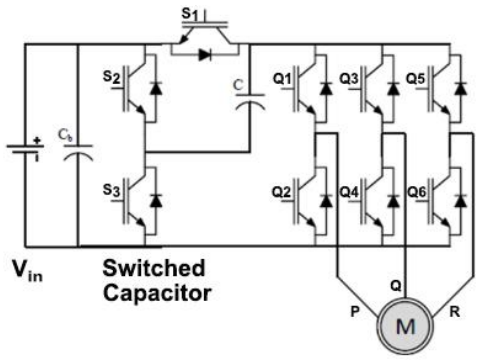

Figure 1a. Block diagram of proposed system

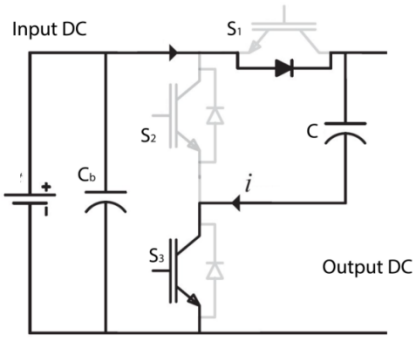

Figure 1b. Charging of SC converter (Mode 1)

When operating in mode I, also known as the charging mode, the monostable circuit's lowermost switch S3 closes, allowing the capacitor to be charged with the supply voltage. Mode I is shown in the circuit of Figure 1b. The uppermost S2 switch closes, and the charged capacitor discharges while operating in mode II. Consequently, both the supply voltage and the capacitor discharge voltages double. The Vout exceeds the Vin. The switching speed of the converter and Vout varies directly. Mode II is illustrated in the circuit of Figure 1c.

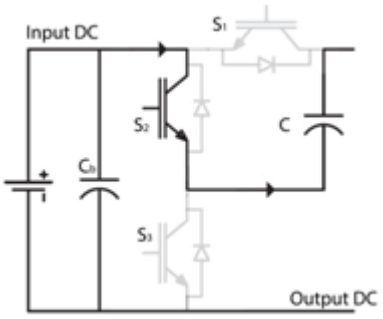

Figure 1c. Discharging of SC converter (Mode 2)

3. Simulation Results and Discussion

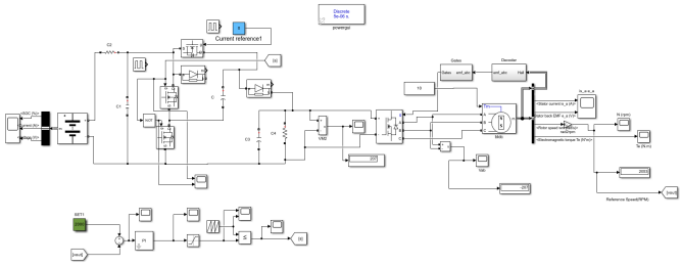

Figure 2. Proposed simulation model

BLDC drive control using MATLAB/Simulink is shown in the figure 2. At the start of the simulation, a PWM signal suitable for BLDC control is generated. Consequently, the controller, which is wired to receive the Hall signal and adjust the motor speed accordingly, can detect the rising and falling edge positions of the BLDC rotor. The controller calculates the rotor speed through combinational logic computation, taking the rotor rising and falling edge positions of the Hall signals as inputs [7]. To enhance the PWM signal according to the BLDC drive, a Hall sensor is used to combine balanced Hall signals with an efficient controller. The speed controller continues to rely on the duty ratio of the efficient PWM signal to regulate the motor speed.

Based on the original pulse-width modulation (PWM) signal and the balanced Hall signals, the torque controller is then used to generate objective-based PWM signals during the secondary stage of the simulation. The logical signal to the H6 inverter is implemented using the microcontroller's logic circuit. On the other hand, while using the high-bridge switching PWM mode, the PWM delay only affects the lower bridge switches [8-11].

As illustrated in figure 3, which depict a smooth transition at the rated speed of 2010 RPM, the duty ratio of the MOSFET switch is adjusted to maintain a constant dc-link voltage, as shown in figure 4. The design of the hybrid input source-fed H6 inverter for controlling the BLDC motor drive was validated using a hardware model [12].

The motor, supplied with an input voltage of 210 V as indicated in figure 5, induces an electromotive force of 75

V. The electromagnetic torque provided by the motor is 12.5 NM for a load current of 1.5 A as shown in figure 6 and 7. The switching frequency of the SC converter is 100 Hz, and the switching frequency of the H6 inverter is 20 Hz, as shown in figure 8. The pulse given to SC converter is as shown in figure 9.

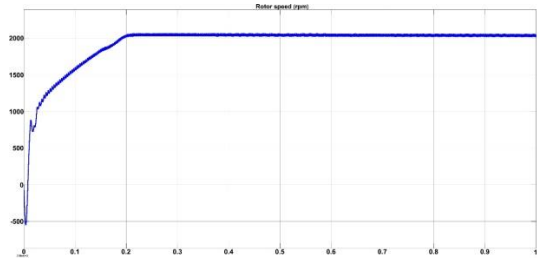

Figure 3. Rotor speed of BLDC motor

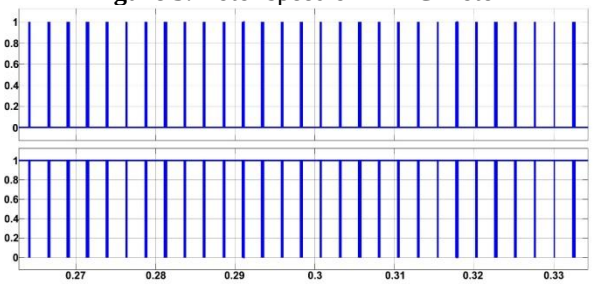

Figure 4. Output voltage of switched capacitor boost converter

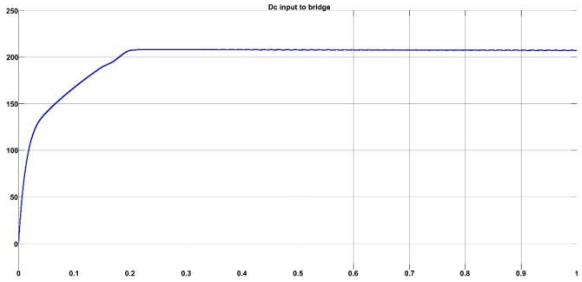

Figure 5. DC input to bridge

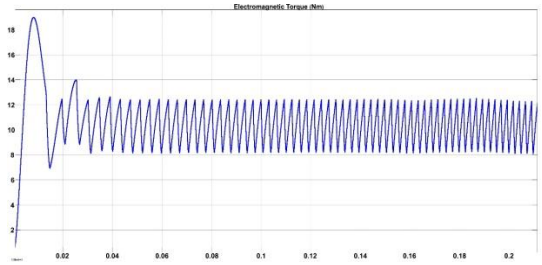

Figure 6. Electromagnetic torque of BLDC motor

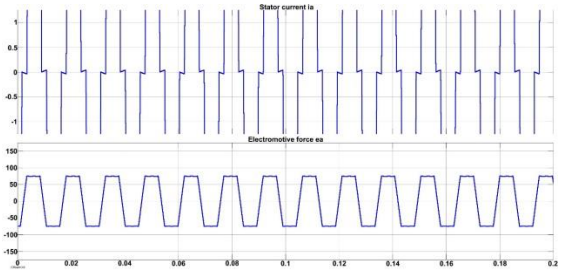

Figure 7. Motor stator current and electromotive force

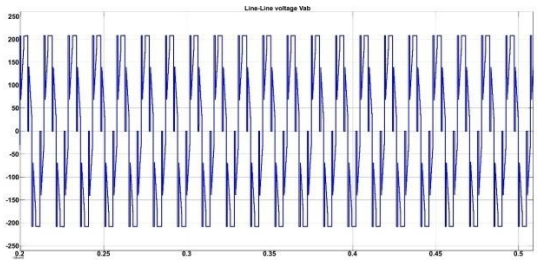

Figure 8. Three phase input to motor

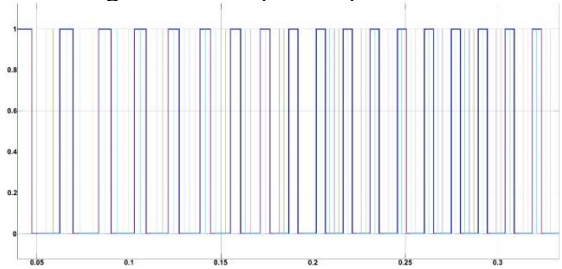

Figure 9. Pulse waveform

4. Hardware Results and Discussion

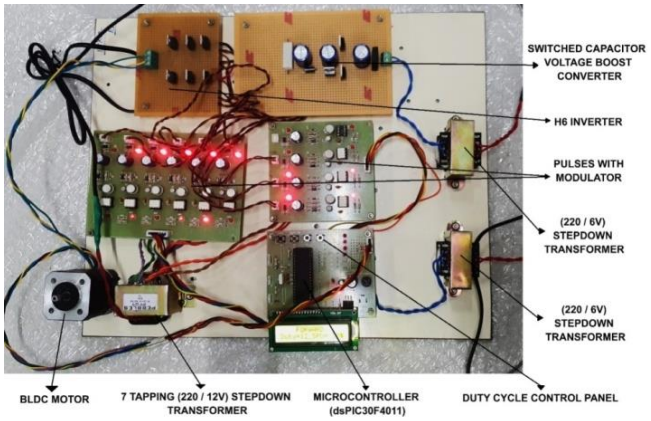

Figure 10. Hardware of Proposed system

The hardware of proposed system is as shown in figure 10. A diode bridge rectifier is used to convert the 230 V input AC voltage to 6 VDC. There is a 6 VDC voltage set. The SC leg's switching frequency is set to 20 kHz, while the inverter legs' switching frequency is set to 10 kHz. The switched-capacitor value is 1000 µF/63 V.

To create a single circuit, the paper combines an inverter and a switched-capacitor circuit. Using the switched-capacitor circuit, a multilevel dc-link voltage is produced. Consequently, the large filtering capacitor and the reverse-blocking diode on the load side are absent from the proposed switched-capacitor circuit, which sets it apart from the conventional one. Unified control of the inverter and switched-capacitor stages enables the regulation of the output voltage and current as indicated in figure 11.

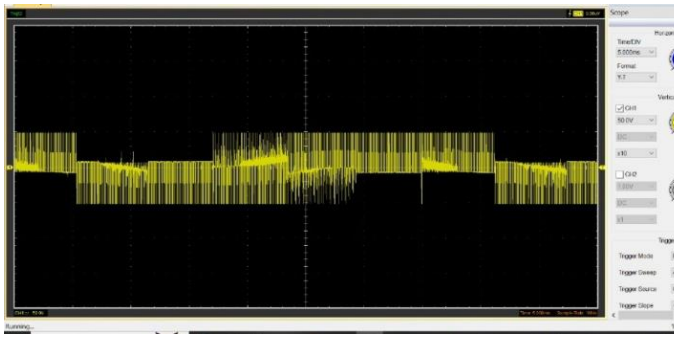

Figure 11. Motor input Voltage

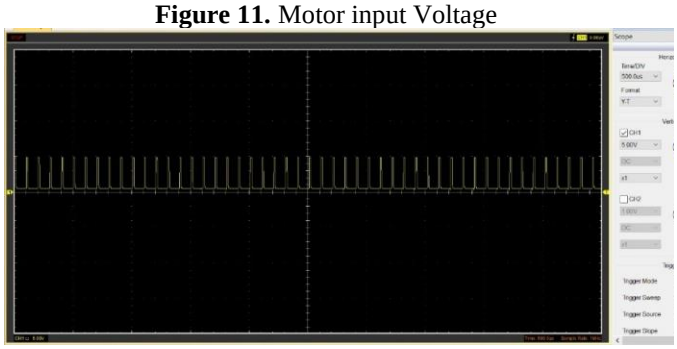

Figure 12. Gate pulses for H6 inverter

The switched-capacitor boost converter converts 6 V DC to 12 V DC. Based on the power balance between the input terminal ports, the suggested controller was provided to the H6 inverter [13].

The figure 12 illustrates the operating gate signals for the higher leg MOSFETs (IRF840) Q1, Q3, Q5, and the lower leg MOSFETs Q2, Q4, Q6. A constant duty cycle for each input source is compared to a trapezoidal signal (reference trapezoid) with the required switching frequency of the H6 inverter at that same frequency. The switch will be in the OFF position if the trapezoidal pulse value is less than the duty cycle and in the ON position otherwise. Switches Q1, Q3, and Q5 conduct in a forward manner toward switches Q2, Q4, and Q6 [14]. Phases P, Q, and R of the alternating current grid are intended to be served by the three-legged bridge. Each leg of the bridge is composed of two anti-parallel MOSFETs driven by complementary pulses [15-17].

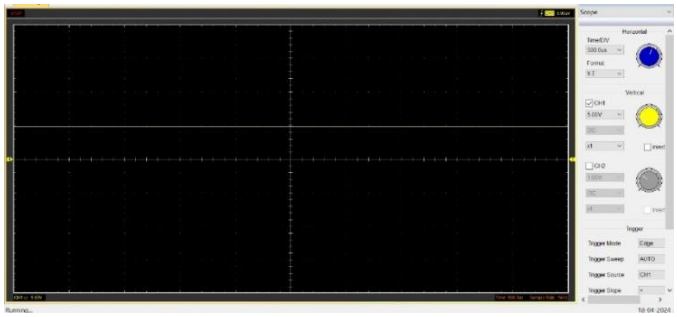

Figure 13. Output voltage of switched capacitor boost converter

Three MOSFETs, one for each leg (P, Q, and R) of the full-bridge circuit, are connected in series with the inductor and are anti-parallel to one another.

To provide sufficient driving pulses for the MOSFETs in the full-bridge circuit, three symmetrical reference waves with a 120-degree phase difference are first created within the control module of the desired dsPIC30F4011 (PWM controller) H6 and fed to the inverter. Driving pulses are generated by comparing the BLDC motor reference signal to zero. To obtain the desired output, the driving pulses for the three-phase bridge switches are produced by turning on each leg of the bridge individually when the corresponding reference signal is equal to or greater than the trapezoidal pulse width [18,19].

The motor was supplied with an input voltage of 10 V. The speed of the BLDC motor was controlled by varying the output voltage of SC converter by adjusting duty cycle as indicated in figure 13. For example, when the duty cycle was 11%, the motor speed was 320 RPM. When the duty cycle was increased to 30%, the speed of the motor was 1000 RPM. When the duty cycle was 50%, the corresponding speed was 1410 RPM. Finally, when the duty cycle was 90%, the maximum speed achieved was 1600 RPM. Table 1 indicates the speed of motor for various duty operations and Table 2 specifies the hardware components used for building the hardware.

Table 1. Duty cycle Vs Speed

S.No	Duty Cycle (%)	Speed (Rpm)
1	11	320
2	30	1000
3	50	1410
4	70	1550
5	90	1600

Table 2. Hardware components and specifications

SNO	Component	Specification	Tasks
1.	MOSFET	IRF840	Used in the switching power supply, motor controlling, inverter
2.	Transformer	220/6V 220/12V - 7 tapping	A Transformer used to reduce the a.c. sources for the power of the board.
3.	Microcontroller	dsPIC30F4011 24 bit wide instructions Operating voltage (3.3v to 5.5v) No. of Pins:40Pins	Used for the PWM generation in the controlling of motor.
4.	Motor	RMCS -1021 (42BLS02) Number Of Phases: 3 Number Of Poles: 8 Rated Voltage: 24 VDC Rated Speed 4000 (Rpm) Rated Torque 0.125 N.m Rated Current 3.3 (Amps)	Motor used for the checking for pulse with modulation sensor in the board.
5.	Capacitor	1000uf (25V), 1000uf (63V)	capacitors is used energy storage, power conditioning, electronic noise filtering
6.	Optical driver	TLP250H Supply voltage : 10-35V Output current : ±1.5A (max) Switching time: 0.5μs(max)	TLP250 provides output from low to high with minimum threshold current of 1.2mA and above.
7.	Simulation	MATLAB/Simulink.	To check the simulation and test results.

5. Conclusion

The proposed circuit approach is tested to significantly enhance the performance of the BLDC motor speed control drive. The findings indicate that the suggested PI-based speed control technique is reliable and effective. In the proposed system, the drive can utilize an input supply voltage and still operate the BLDC motor at its rated specifications. The H6 Voltage Source Inverter receives an optimized PWM signal from the torque controller drive system. It is evident that the proposed circuit methodology substantially improves the stability and performance of the BLDC drive. The BLDC motor achieves its optimal rated speed through the proposed PI controller drive, and the results are analysed and validated.

References

1. A. Ioinovici, "Switched-capacitor power electronics circuits," IEEE Circuits and Systems Magazine, vol. 1, issue 3, pp. 37-42, 2020.

2. C. Barth, I. Moon, Y. Lei, S. Qin, R.C.N. Pilawa-Podgurski, "Selection of capacitors for power buffering in single-phase inverter applications," in Proc. IEEE Energy Conversion Congress and Expo, 2021.

3. J. W. Kimball and P. T. Krein, "Analysis and design of switched capacitor converters," in Proc. IEEE Applied Power Electronics Conf., 2020, pp. 1473-1477.

4. Y. Lei and R.C.N. Pilawa-Podgurski, "Soft-charging operation of switched-capacitor DC-DC converters with an inductive load," in Proc. IEEE Applied Power Electronics Conf., 2020, pp. 2112-2119.

5. B.B. Macy, Y. Lei, and R.C.N. Pilawa-Podgurski, "A 1.2 MHz, 25 V to 100 V Gan-based resonant Dickson switched-capacitor converter with 1011 W/in3 (61.7 kW/L) power density," in Proc. IEEE Applied Power Electronics Conf., 2021, pp. 1472-1478.

6. Y. Lei and R.C.N. Pilawa-Podgurski, "A General Method for Analyzing Resonant and Soft-Charging Operation of Switched-Capacitor Converters," IEEE Trans. Power Electronics, vol. 30, issue 10, pp. 5650-5664, 2019.

7. R.C.N. Pilaf-Podgurski and D.J. Perreault, "Merged Two-Stage Power Converter With Soft Charging Switched-Capacitor Stage in 180 nm CMOS," IEEE Journal of Solid-State Circuits, vol. 47, issue 7, pp. 1557-1567, 2021.

8. C. Schaef, K. Kesarwani, and J.T. Stauth, "20.2 A variable

conversion-ratio 3-phase resonant switched capacitor converter with 85% efficiency at 0.91W/mm2 using 1.1nH PCB-trace inductors," in Proc. IEEE Solid-State Circuits Conf., 2021.

9. F. Z. Peng, F. Zhang, and Z. Qian, "A magnetic-less DC-DC converter for dual-voltage automotive systems," IEEE Trans. Industry Applications, vol. 39, pp. 511-518, March-April 2020.

10. M. Shen, F. Z. Peng, and L. M. Tolbert, "Multilevel DC–DC power conversion system with multiple DC sources," IEEE Trans. Power Electronics, vol. 23, pp. 420-426, January 2019.

11. L. Fu, X. Zhang, F. Guo, and J. Wang, "A phase shift controlled current-fed Quasi-Switched-Capacitor isolated dc/dc converter with GaN HEMTs for photovoltaic applications," in Proc. IEEE Applied Power Electronics Conf., 2021, pp. 191-198.

12. Y. Cao and Z. Ye, "Simulation and analysis of switched capacitor dc-dc converters for use in battery electric vehicles," in Proc. IEEE Power and Energy Conf. at Illinois, 2019.

13. X. Chen, et al., "An overview of lithium-ion batteries for electric vehicles," in Proc. IEEE Power and Energy Conf., 2021, pp. 230-235.

14. B. Bural, et al., "An experimental comparison of different topologies for fuel-cell, battery and ultra-capacitor in electric vehicle," in Proc. IEEE National Conf. on Electrical, Electronics, and Computer Engineering, 2019, pp. 46-52.

15. R. C. Kroeze and P. T. Krein, "Electrical battery model for use in dynamic electric vehicle simulations," in Proc. IEEE Power Electronics Specialists Conf., 2020, pp. 1336-1342.

16. Y. Cao and P. T. Krein, "An average modeling approach for mobile refrigeration hybrid power systems with improved battery simulation," in Proc. IEEE Transportation Electrification Conf., 2019.

17. [Online]. Available: http://articles.sae.org/12833/

18. P. C. Krause, O. Wasynczuk, and S. D. Sudhoff, Analysis of Electric Machinery and Drive Systems, 2nd ed. Edison, NJ: Wiley-IEEE Press, 2022, pp. 525-556.

19. M. Seeman and S. R. Sanders, "Analysis and optimization of switched capacitor dc-dc converters," IEEE Trans. Power Electronics, vol. 23, no. 2, pp. 841-851, March 2020.